

HYBRID MICROOPTICAL WDM RECEIVER FOR PON COMMUNICATION

Vitezslav JERABEK¹, Julio ARMAS¹, Vaclav PRAJZLER¹

¹Department of Microelectronics, Faculty of Electrical Engineering, Czech Technical University in Prague, Technicka 2, 166 27 Prague, Czech Republic

jerabek@fel.cvut.cz, armas@fel.cvut.cz, prajzler@fel.cvut.cz

Abstract. The paper presents the design, simulation and construction results of the wavelength division multiplex (WDM) optical hybrid receiver module for the passive optical network (PON). The optical WDM receiver was constructed using system of three micromodules in the new circle topology. The optical micromodule contains multimode fiber pigtail 50/125 μm , VHGT filter with collimation lens and two microwave optoelectronics receiver micromodules (OE receiver micromodules). OE receiver micromodules were designed by use small signal equivalent electrical circuit model and noise model, from which the mathematically solved the transmittance function, which was used for calculation and simulation of the optimal frequency characteristics and signal to noise ratio. For determine the limit frequency of OE receiver micromodule, the transcendent equation with transmittance function was numerically solved. OE receiver micromodule was composed of decollimation lenses and microwave optoelectronics receivers with bandwidth 2,5 GHz and alternatively in SMD technology with bandwidth 1,25 GHz, using the thin layer hybrid technology. WDM receiver use radiation 1490 nm for internet and 1550 nm for digital TV signals download information.

Keywords

Collimating lens, microoptical hybrid integration, Volume holographic grating triplexer, WDM Receiver.

1. Introduction

The micromodules for WDM receiver are considered to be the key component for realizing fiber-to-the-home networks. Especially an optical WDM Receiver module, that can receive a 1490 nm download data as well as a 1550 nm download video signals for cable TV applications. A microoptical lightwave hybrid integration technology enables us to construct a microoptical

integrated lightwave circuits (MLC) and planar integrated lightwave circuits (PLC) by combining components with passive function (optical fiber, lens, VHGT (volume holographic grating triplexer), planar optical waveguides and active optoelectronics devices (laser diodes, optical amplifiers and photodiodes) hybridized on one substrate for collimating, focusing, imaging, branching, receiving and transmitting of an optical beams [1], [2].

WDM receiver, Fig. 1, was constructed by using system of three micromodules set on the substrate in the new circle topology [3]. The optical demultiplexing micromodule is created by multimode optical fiber, collimating lens and volume holographic grating triplexer diffraction filter (VHGT) [4] and the two type microwave optoelectronic receiver micromodules (OE receiver micromodules) with bandwidth 2,5 GHz or 1,25 GHz. In the OE receiver micromodules, each diffracted beam from VHGT was focused on the active area of PIN photodetector (PIN PD) connected to microwave amplifier. The microoptical WDM receiver system will be assembled in DIL case.

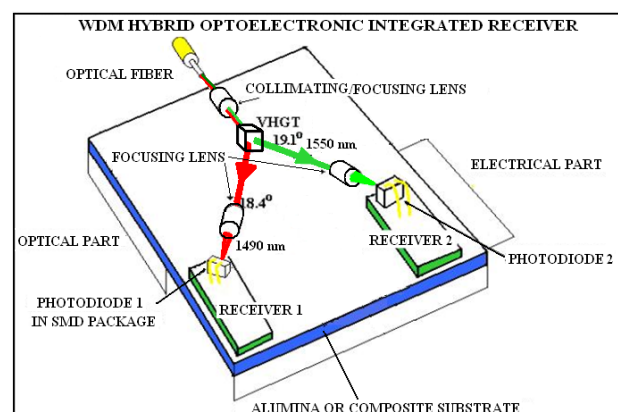


Fig. 1: WDM Receiver optical system with VHGT.

2. System Design and Measurement of Optical Micromodule

The OE micromodule is represented by the block diagram

shown in Fig. 2. A special cylindrical lens is used in the WDM receiver to collimate the beam before the VHGT. The VHGT surface is covered antireflection layers. The collimated beam is diffracted by the VHGT and focused on the active area of PIN photodiodes by collimation lenses. The PIN PD converts the received optical power of the radiation into a photocurrent [5].

We analyze the optical system and calculate parameters of the optical micromodules - focal lengths and insertion losses of the lenses, angles of diffraction, diffraction efficiency, diffraction crosstalk on the VHGT for the wavelengths 1490 nm and 1550 nm.

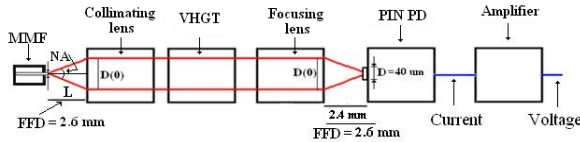


Fig. 2: Block diagram of WDM receiver signal path.

2.1. Analyses of Optical Collimating/Focusing System

WDM receiver high efficiency optical system uses collimating/focusing lenses for optical processing of the beam and spot transformation. The radiation propagates from the multi mode fiber (MMF) across the first collimating lens, VGHT and focusing lenses on the active area of the PIN PD's connected by microstrip electrical waveguides to the input of the electronic amplifiers. The main parameters of the system were the optical angles, focal distance of the lenses and the diameter of the beam spots, which had a significant influence on VHGT optical characteristics (diffraction efficiency, optical crosstalks, sensitivity etc.).

The optical analysis by ray-transfer matrix describes optical systems in the paraxial approximation. The ray-transfer matrix (S_1) is used in order to find simple and explicit expressions for determination of the beam optimal structural parameters of the focusing system. The modal field profiles in the MMF and collimating lenses are assumed, to be circular symmetric and Gaussian and consider the propagation of a ray in a homogeneous medium [6]. The schema of the collimating system composed of the MMF and the collimating lens is shown in Fig. 3.

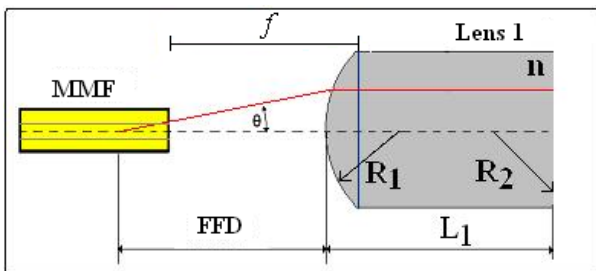


Fig. 3: Collimation system: MMF-cylindrical lens L_1 . (FFD – front focal distance, L_1 - length of the collimating lens, R_1 , R_2 - radius of curvature of the lens, n_2 - refractive index, f – focal length, θ angle of numerical aperture.

The ray – transfer matrix (S_1) of the collimating lens was calculated as the multiplication of the translation matrix T_1 and the refraction matrices M_1 and M_2 shown in formulas (1), (2) and (3).

$$S_1 = M_1 T_1 M_2, \tag{1}$$

$$S_1 = \begin{bmatrix} 1 & 0 \\ -\frac{n_2-1}{R_1} & 1 \end{bmatrix} \begin{bmatrix} 1 & L_1 \\ 0 & 1 \end{bmatrix} \begin{bmatrix} 1 & 0 \\ -\frac{n_2-1}{R_2} & 1 \end{bmatrix}, \tag{2}$$

$$S_1 = \begin{bmatrix} 1 - P_1 t & t \\ -P_1 - P_2 + P_1 P_2 t & 1 - P_2 t \end{bmatrix} = \begin{bmatrix} A & B \\ C & D \end{bmatrix}, \tag{3}$$

where P_1 , P_2 and t are defined by (4), (5) and (6).

$$P_1 = \frac{n_2 - 1}{R_1}, \tag{4}$$

$$P_2 = \frac{n_2 - 1}{R_2}, \tag{5}$$

$$t = \frac{L_1}{n_2}. \tag{6}$$

The focal plane of the collimating lens is defined by (7).

$$\begin{bmatrix} 0 \\ \beta_{out} \end{bmatrix} = \begin{bmatrix} 1 & b \\ 0 & 1 \end{bmatrix} \begin{bmatrix} A & B \\ C & D \end{bmatrix} \begin{bmatrix} y_{in} \\ 0 \end{bmatrix}, \tag{7}$$

this implied that

$$0 = (A + b \cdot C) y_{in}, \tag{8}$$

therefore

$$b = -\frac{A}{C}, \tag{9}$$

where b is the front focal distance FFD of the lens defined by (10), β_{out} is output angle and y_{in} is the input radial position of the ray.

$$FFD = b = -\frac{1 - P_1 t}{-P_1 - P_2 + P_1 P_2 t}. \tag{10}$$

The parameters of the optical system are: $L_1 = 3,0$ mm, $R_1 = 2,3$ mm, $R_2 = \infty$ (the concave radius of curvature of lens back surface). The calculated values of FFD and attenuation in the collimating lens due to Fresnel reflection at the interfaces A_F for different wavelength are shown in the Tab. 1.

Tab.1: The calculated values of the collimating lenses and optical attenuation for the wavelength 1310, 1490 and 1550 nm.

λ [nm]	n	FFD [mm]	A_F [dB]
1550	1,4865	2,493	0,32903
1490	1,4870	2,488	0,33956
1310	1,4885	2,476	0,34129

The decollimation lens in the optoelectronic micromodule is to provide optimal radiation focus of the diffracted beam on the active space of PIN PD.

The radio y of the beam exposition to the active area of PIN PD depends on the distance z between the decollimation lens PIN PD and the diameter of the beam $D(0)$. With the formula (11), we obtain the radio of the active area covered.

$$y = -m \cdot z + q = -\frac{D(0)}{2 \cdot FFD} \cdot z + \frac{D(0)}{2}, \quad (11)$$

where: y is the radio of the active area, m is the slope of a line, q is the diameter of the beam at $z = 0$ mm, $D(0)/2$ is the half diameter of the beam at $z = 0$ mm.

To cover all the active area of the PIN PD the distance between the decollimation lens and PIN PD dependence is shown in Fig. 4.

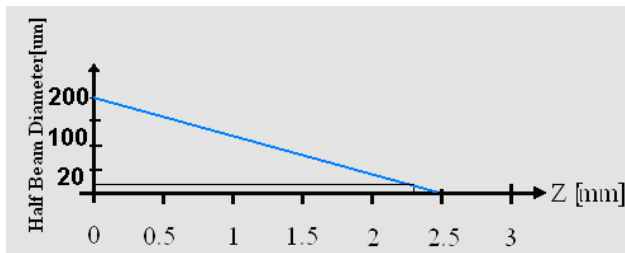


Fig. 4: Half beam diameter $D(0)/2$ in function of distance z .

For the focusing process, it was important to analyze the active area of the PIN PD covering by the radiation cone, formed behind focusing lens. For the diameter active area $D = 40 \mu\text{m}$ of PIN PD was calculated and measured distance from the focusing lens $FFD = 2,34$ mm.

2.2. Analysis and Measurement of VHGT

For the optical demultiplex of the wavelength 1490 nm and 1550 nm optical beam in WDM receiver was in the optical micromodule used the VHGT filter from Ondax Ltd. with double grating system. This transmission type grating filters has high diffraction efficiency, very low insertion losses and optical crosstalk.

The Bragg diffraction condition is given by (12)

$$\lambda_B = 2 \cdot \Lambda \sin\left(\frac{\theta_{diff}}{2}\right), \quad (12)$$

where Λ is Bragg constant, λ_B is the Bragg wavelength, θ_{diff} is the diffraction angle.

From Eq. (12) were determined Bragg constants of VHGT by use measurement of the diffract angle. The Bragg constant $\Lambda = 4,66 \mu\text{m}$ and $\Lambda = 4,671 \mu\text{m}$ was calculated, where $\theta_{diff} = 18,4^\circ$ for $\lambda_1 = 1490$ nm and $\theta_{diff} = 19,1^\circ$ for $\lambda_2 = 1550$ nm.

The Bragg diffraction efficiency η_B for VHGT was defined as the ratio between the diffracted intensity and the incident intensity, without considering absorption and Fresnel reflections at the interfaces. When the Bragg condition is satisfied for wavelength λ_B , the diffraction efficiency η_B is given for transmission gratings first

diffraction order [4] as (13).

$$\eta_B = \sin^2\left(\frac{\pi \cdot n_1 \cdot D}{\lambda_B \cos \theta_n}\right), \quad (13)$$

where θ_n is the Bragg-matched incident angle in the medium, n_1 is grating strength refraction index modulation, D is the thickness of the grating, and λ_B is the Bragg wavelength. For the compromise position of both gratings VHGT systems, the diffraction efficiencies were calculated as 71,0 % and 74,9 % for 1550 nm and 1490 nm respectively. The space distribution of VHGT optical beams are shown in Fig. 5 and the measured values are shown in Tab. 2.

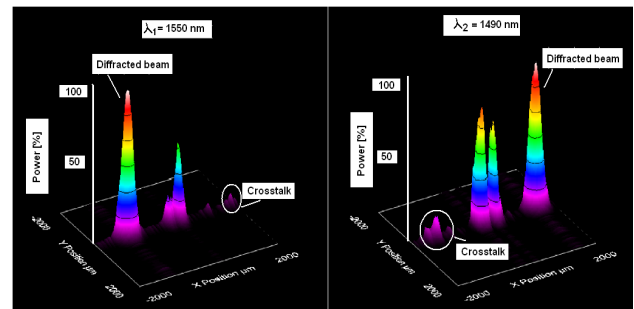


Fig. 5: The diffracted beams with crosstalk at wavelength $\lambda_1 = 1550$ nm and $\lambda_2 = 1490$ nm.

Tab.2: The measured diffraction efficiency η_B and diffraction losses A_F of the VHGT.

λ [nm]	P_{IN} [μW]	P_D [μW]	η_B [%]	A_F [dB]
1550	367	268,7	73,21	1,35
1490	879	659	75,0	1,24

Where P_{IN} is incident optical power, P_D is diffracted optical power and A_F [dB] is the attenuation in the VHGT due to non diffracted beam and crosstalk. The attenuation in the VHGT due to Fresnel reflection at the interfaces is very low because the VHGT has antireflection coated surfaces.

By the measurement, the space distribution of an optical power was investigated that in the center of diagram Fig. 5, exist two peaks of radiation no diffracted, which don't equal of Bragg condition. These radiations have to be filtered, when VHGT will be used in three wavelength WDM receiver or transceiver. At the opposite side of the space distribution power diagram is clear perceptible peaks diffracted to the opposite direction as optical crosstalk. In the next measurement of optical crosstalk was used the formula (14).

$$A_\lambda = 10 \log\left(\frac{P_{1\lambda}}{P_{2\lambda}}\right), \quad (14)$$

where $P_{1\lambda}$ is the is the optical diffracted power, $P_{2\lambda}$ is optical power second wavelength, diffracted at the same direction than $P_{1\lambda}$.

The minimal optical crosstalk of the optical beams for two wavelengths was very important requirement for

the good BER (bit error rate). The optical crosstalk was given by optical power, which was diffracted to wavelength opposite direction. For BER = 10⁻⁹ it was needed optical crosstalk attenuation $A_\lambda > 11$ dB. The optical crosstalk $P_{2\lambda}$ for the wavelength $\lambda_1=1490$ and $\lambda_2 = 1550$ nm with the total power normalized to $P_{IN} = 360 \mu\text{W}$ was measured. It correspond $A_\lambda = 18,29$ dB and 12,44 dB as is shown in Tab. 3.

Tab.3: The optical crosstalk of the VHGT beams measurement.

λ [nm]	Total Power P_{IN} [μW]	Diffracted Power $P_{i\lambda}$ [μW]	Crosstalk $P_{2\lambda}$ [μW]	A_i [dB]
1550	360	268,7	15 ₁₄₉₀	12,44
1490	360	659	4 ₁₅₅₀	18,29

For measurement of the optical power space distribution in 2D or 3D was used beam profiler head BP 104 IR from Thorlabs with special software. The crosstalk measurement show us that using the VHGT is possible diffract two beams at the same time without undesired effect from each other.

3. System Design and Measurement of OE Receiver Micromodules

For OE receiver micromodules were used two types of the OE receivers. For construction of the 1,25 GHz optoelectronic microwave micromodules with transimpedance OE receiver was used SMD technology, which is sufficient for this dynamics response devices. OE receivers were designed by use small signal equivalent electrical circuit model and noise model. The internal structure of the transimpedance OE receiver, with the ATF-36163 amplifier, InGaAs PIN photodiode and the bias circuitry is presented in Fig. 6. All components - PIN PD, capacitors, resistors and inductance in SMD package were assembled on composite low loss substrate (Rogers), with Au/ Cu microstrip line and waveguide motive. The focusing lens was fixed on Au/ Cu carrier in front of PIN PD.

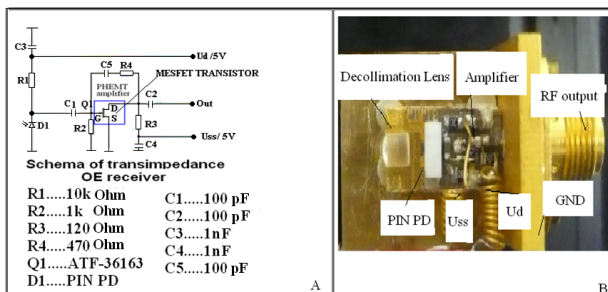


Fig. 6: Design and construction of OE receiver micromodule. A) The electrical schema of the transimpedance OE receiver B) The real microwave optoelectronic micromodule assembly.

The low impedance OE receiver for 2,5 GHz bandwidth optoelectronic micromodules were realized by the thin layer hybrid integration technology. For realized

OE receiver micromodules, the electro/optical transmission, dynamic response and noise figure characteristics parameters were designed and measured. The low impedance OE receiver was composed of the InGaAs PIN photodetector C30616 ECER with bandwidth 3,5 GHz and HBT monolithic amplifier HM 396 made by GaAs/ InGaP heterojunction bipolar transistors technology (HBT) with bandwidth 8GHz and gain 20 dB. In microwave signal path was used a microstrip waveguide, connecting the PIN PD to the signal input of HBT amplifier. The thin film Au microstrip waveguides was formed by a standard lithographic sputtering process assembly on an alumina substrate, in which the passive and active components in chip form are mounted directly on Au strip waveguide lines and fix by epotek. The parameters of WDM receiver were calculated and measured. The low frequency transmittances were 140 V/W and 170 V/W for low and transimpedance OE receivers respectively. The dynamic measurement results of modulation frequency characteristic OE receivers, $f_T = 2,5$ GHz for low impedance OE receiver and $f_T = 1,25$ GHz for transimpedance OE receiver as is shown in Fig. 7.

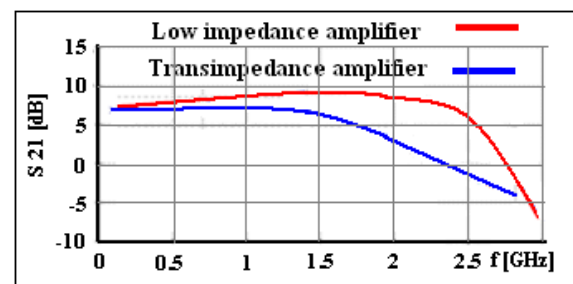


Fig. 7: The measured scattering parameter S_{21} frequency characteristics of the OE receiver for low impedance and transimpedance amplifier.

The signal to noise ratio (SNR) of WDM receiver was calculated and measured for both type of OE receivers. In the case of the transimpedance OE receiver was measured SNR = 27,3 dB and in the case of the low impedance OE receiver SNR = 23,6 dB. This corresponds with optical attenuation reserves 5,7 dB for transimpedance and 2 dB for low impedance OE receiver. We presume SM fiber with an optical loss 0,2 dB/km and SNR = 21,6 dB for BER = 10⁻⁹. These values correspond to the transmission distance of the 28,5 km or 10 km optical SM fiber. When we subtract optical losses 1,4 dB of the optical demultiplexing and imagin system of WDM receiver, the transmit distance drop to 21,5 km or 3 km of optical SM fiber respectively. The WDM receiver Rx has been constructed using system of three micromodules in the new circle topology set on the alumina or composite substrate. The fundamental layout of the hybrid integrated microoptical WDM receiver is given on Fig. 8.

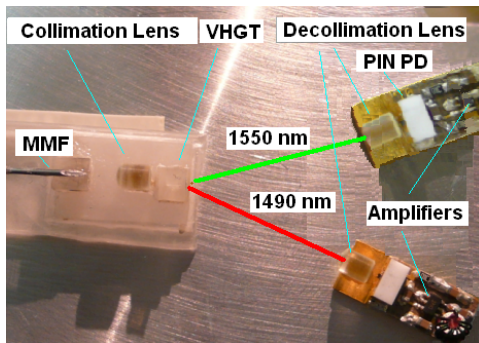


Fig. 8: WDM receiver micromodule layout based on microoptical hybrid integration technology.

4. PLC Hybrid Integrated WDM Transceiver

WDM transceiver in PLC (Planar Lightwave Circuit) hybrid integration technology is shown in Fig. 9. Our work was focused on design an optical part of WDM receiver, which was realized as PLC triplex filter designed by two stage multimode interference or microring resonator filter, which was made from polymer materials. For design was used BMP program from R Soft. As polymer we choose NANOTM SU-8 2000 polymer from Micro Chem Corp. due to good optical and mechanical properties (this polymer has optical losses less than 1 dB/cm for 1300 and 1550 nm wavelengths).

The polymer layer was deposited by using spin coating method with silica on silicon substrate. Before application of lithography procedure, the samples were prebaked at 90 °C for 45 min before a lithography. As a last step, the post backing at 90 °C for 60 min would be applied. The channel waveguides would be fabricated by using UV light for carried out of the stabilized optical properties. The photodetectors and laser in SMD package were placed in the groove for elimination height offset.

The optimum distance among optical waveguides facet on base polymer SU8-2000 and optical fiber or photodetector in the receiving part was specified by BMP program simulation. The receive optoelectronic part was made same as at microoptical type WDM receiver. The optoelectronic transmitter for $\lambda_3 = 1310$ nm upstream radiation uses Fabry-Perot InGaAsP laser diode fix on metallic submount with a microwave modulator and optical average power feedback control electronics. The feedback control was realized by ADN 2830A integrated circuit from Advance Semiconductor. The optical microisolator and collimation lens separate laser diode from nondiffracted radiation of the VHGT downstream beams.

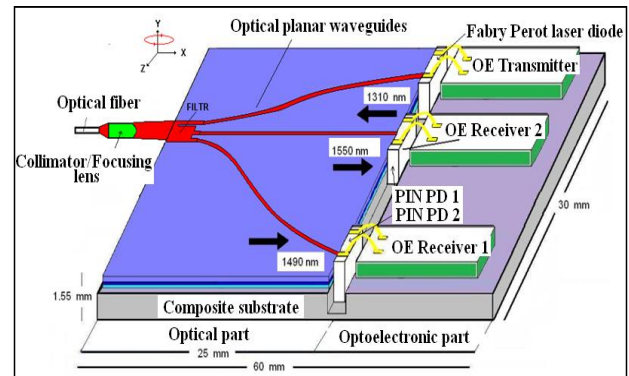


Fig. 9: WDM planar hybrid integrated transceiver.

5. Conclusion

The paper presents design a novel topology and technology solution of IC microoptical hybrid integrated WDM receiver, composed of the optical and optoelectronic micromodules. The optical micromodule use volume holographic grating triplexer (VHGT) as unique optical multiwavelength demultiplexing element in WDM microsystem. The downstream microoptical imagine system was verified by construction and measurement of the microoptical hybrid integrated WDM receiver. Very low insertion optical losses and optical crosstalk of VHGT element imply the high sensitivity and the transmit distance of optical SM fiber. Further work was concentrated on design and construction of WDM transceiver realized by planar lightwave circuit hybrid integration technology. The optical part will be solved by polymer or glass interference filter or microoptical resonators.

Acknowledgements

This research has been supported by grant MPO-TIP FR-TI3/797 and the research program MSM6840770014 of the Czech Technical University in Prague.

References

- [1] KATO, K. and Y. TOHMORI. PLC hybrid integration technology and its application to photonic components. *IEEE Journal of Selected Topics in Quantum Electronics*. 2000, vol. 6, iss. 1, pp. 4-13. ISSN 1077-260X. DOI: 10.1109/2944.826866.
- [2] HATTA, T., T. MIYAHARA, N. OKADA, M. ISHIZAKI, M. NAKAJI, E. ISHIMURA and K. MOTOSHIMA. Hybrid Integration of Waveguide Photodiode and Preamplicifier IC Using Au Stud Bump. *Journal of Lightwave Technology*. 2006, vol. 24, no. 8, 3187–3194. ISSN 0733-8724. DOI: 10.1109/JLT.2006.878044.
- [3] ARMAS, J., V. JERABEK, K. BUSEK, D. MARES and V. PRAJZLER. Microoptical Triplexer System with High

- Efficiency for WDM Hybrid Optoelectronic Receivers. In: *Proceeding of the Electronic Devices and Systems IMAPS CS International Conference*. Brno: Brno University of Technology, 2010, pp. 126-128. ISBN 978-80-214-4138-5.
- [4] Volume Holographic Gratings (VHG). In: *Ondax, Inc.* [online]. 2005. Available at: <http://www.ondax.com>.
- [5] JUDSON TECHNOLOGIES. *PIN PD J22-CO2-RO 40U: Technical documentation*. 2003. Available at: <http://pdf.directindustry.com>.
- [6] MENZEL, R. *Photonics*. Berlin: Springer, 2007. ISBN 978-3540451587.
- [7] HAN, Y.-T., Y.-J. PARK, S.-H. PARK, J.-U. SHIN, C.-W. LEE, H. KO, Y. BAEK, C.-H. PARK, Y.-K. KWON, W.-Y. HWANG, K.-R. OH and H. SUNG. Fabrication of a TFF- Attached WDM-Type Triplex Transceiver Module Using Silica PLC Hybrid Integration Technology. *Journal of Lightwave Technology*. 2006, vol. 24, no. 12, pp. 5031-5038. ISSN 0733-8724. DOI: 10.1109/JLT.2006.885001.

About Authors

Vitezslav JERABEK was born in Prague 1951. He received his M Sc and Ph.D. in the Microelectronics from the Czech technical university in Prague 1975, and 1987. From 2005 is head of optoelectronics group at

Department of Microelectronics of the Czech Technical University in Prague. His research interests include planar hybrid integrated optics and optoelectronics devices, modules and systems design, technology and measurement.

Julio ARMAS was born in Ecuador in 1973. In 2000, he graduated in Electronics and telecommunications from the Escuela Politecnica Nacional in Quito –Ecuador. He is currently working as a Ph.D. in the Optoelectronics group. His work is concentrated on the design and construction of microwave optoelectronics transmitters and receivers.

Vaclav PRAJZLER was born in 1976 in Prague, Czech Republic. In 2001 he graduated from the Faculty of Electrical Engineering at the Czech Technical University in Prague at Department of Microelectronics. Since 2005 he has been working at the Czech Technical University in Prague, Faculty of Electrical Engineering, Department of Microelectronics as a research fellow. In 2007 he obtained the Ph.D. degree from the same university. His current research is focused on fabrication and investigation properties of the optical materials for photonics and integrated optics.